[Bis(3-ammonium-1-hydroxypropylidene-1,1-bisphosphonato)iron(II)]: The Fe^{2+} Salt of Pamidronate, a Clinically Effective Diphosphonate Ligand

Khalid Abu-Shandi and Christoph Janiak

Institut für Anorganische und Analytische Chemie, Universität Freiburg, Albertstr. 21, D-79104 Freiburg, Germany

Reprint requests to Prof. Dr. C. Janiak. Fax: +49(0)761-2036147. E-mail: janiak@uni-freiburg.de

Z. Naturforsch. **60b,** 1250 – 1254 (2005); received September 22, 2005

Dedicated to Professor Gerhard Thiele on the occasion of his 70th birthday

The solvent-free title compound $^2_\infty$[Fe^{II}{$H_3N^+CH_2CH_2C(OH)(PO_3H^-)(PO_3H^-)$}$_2$] was prepared by hydrothermal synthesis and consists of (4,4)-nets of iron octahedra (as the nodes) linked by corner sharing tetrahedra of the phosphonate groups. These layers are stacked in an ABB'A' sequence and are connected to give a three-dimensional network by hydrogen bonds between the non-Fe-bridging phosphonate groups. Pamidronate, $C_3H_{10}NO_7P_2^-$ is a zwitterion with an overall charge of −1.

Key words: Iron(II), Diphosphonate, Pamidronate, Hydrogen Bonding, Hydrothermal Synthesis

Introduction

Increased attention has been paid to transition metal (organo)phosphonates in recent years due to their potential applications in ion exchange, absorption, and sensors [1 – 3]. This interest extends to metal *di*phosphonates. Cobalt and iron diphosphonates are also investigated for their magnetic properties [4, 5]. Metal organophosphonates are an extensive class of organic-inorganic hybrid materials [6] with a wide variety of structural motifs including clusters, layers and networks. Attaching additional functional groups such as carboxylate, hydroxyl or amino to the phosphonic acid promises tunable functionality and synthesis tailored towards applications. Such modified diphosphonates also play a role in biological systems, including the removal of iron from iron proteins [7]. The compound 3-ammonium-1-hydroxypropylidene-1,1-bisphosphonate (= pamidronate) as the disodium salt is used clinically in the diagnosis and treatment of diseases affecting bone tissue [8 – 11]. The synthesis and crystal structure of Fe^{2+} pamidronate is reported in this communication.

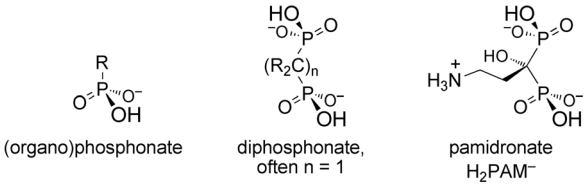

Scheme 1.

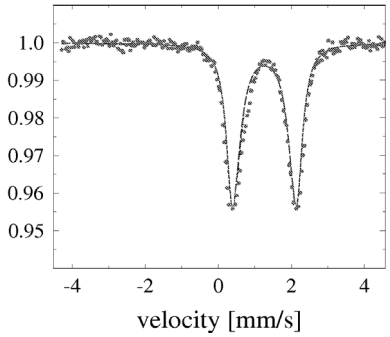

Fig. 1. Mößbauer spectrum of **1** at room temperature. Lorentzians (solid line, parameters in text) are used to fit the experimental data (dots).

Results and Discussion

The Fe^{2+} salt of pamidronate, $^2_\infty$[bis(3-ammonium-1-hydroxypropylidene-1,1-bisphosphonato)iron(II)] or $^2_\infty$[$Fe(H_2PAM)_2$] (**1**) is obtained from sodium pamidronate monohydrate and iron(II) chloride in water under argon and hydrothermal conditions. The compound forms brownish-red to violet crystal plates without solvent of crystallization. The oxidation state +2 for iron in **1** is supported by a Mößbauer measurement (Fig. 1) which at room temperature shows

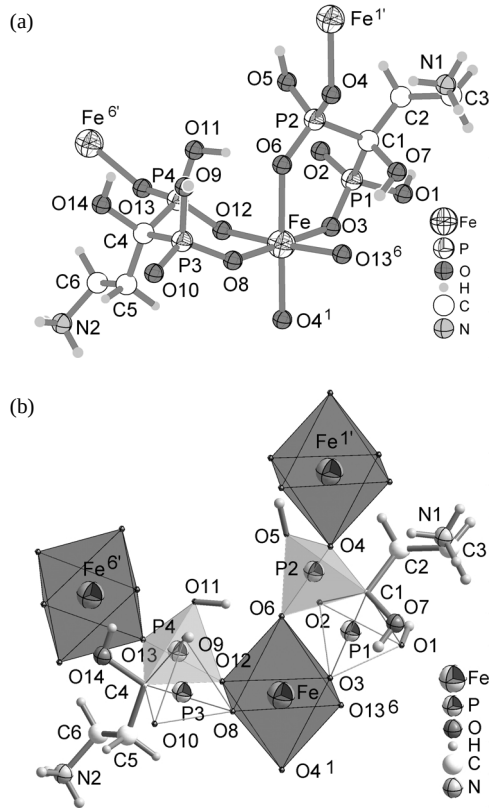

Fig. 2. Formula unit of **1**, with the central iron atom and the two chelating pamidronate ligands. The Fe coordination sphere is completed by oxygen atoms ($O4^1$, $O13^6$) from two bridging phosphonate groups. This bridging action is emphasized by showing the symmetry related iron atoms $Fe^{1'}$ and $Fe^{6'}$. (a) Ball and stick representation, (b) Polyhedral representation (with O atoms contracted) around the Fe and P atoms which leaves only the ammonium-1-hydroxypropylidene residues and the (P-)OH groups as ball and stick drawings. Bridging phosphonate groups (with P2 and P4) are shown with light grey faces, non-bridging phosphonates groups (with P1 and P3) are drawn only with the outline of the tetrahedral skeleton. Selected distances (Å) and angles (°): Fe–O3 2.026(4), Fe–$O4^1$ 2.155(4), Fe–O6 2.238(4), Fe–O8 2.089(4), Fe–O12 2.091(4), Fe–$O13^6$ 2.065(4), O3–Fe–$O4^1$ 88.7(2), O3–Fe–O6 88.1(2), O3–Fe–O8 177.0(2), O3–Fe–O12 91.6(2), O3–Fe–$O13^6$ 85.8(2), $O4^1$–Fe–O6 176.6(2), $O4^1$–Fe–O8 93.0(2), $O4^1$–Fe–O12 88.7(2), $O4^1$–Fe–$O13^6$ 93.4(2), O6–Fe–O8 90.2(2), O6–Fe–O12 90.30(2), O6–Fe–$O13^6$ 87.5(2), O8–Fe–O12 90.9(2), O8–Fe–$O13^6$ 91.6(2), O12–Fe–$O13^6$ 176.6(2); symmetry relations $1 = x, -1+y, z$; $1' = x, 1+y, z$; $6 = x, 1-y, 0.5+z$; $6' = x, 1-y, -0.5+z$.

a doublet with an isomer shift, $\delta^{\alpha-\mathrm{Fe}} = 1.26$ mm/s, and a quadrupole splitting, $\Delta E_\mathrm{Q} = 1.71$ mm/s. At 77 K these values increase to $\delta^{\alpha-\mathrm{Fe}} = 1.40$ mm/s and

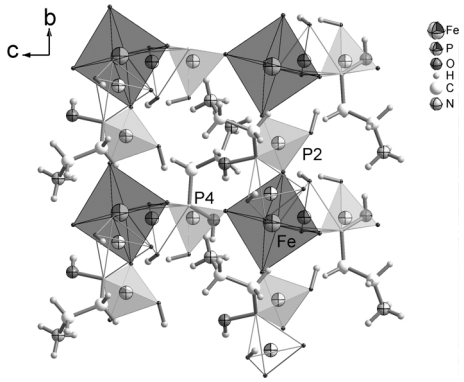

Fig. 3. Section of an individual layer in **1**. Polyhedral representation (with O atoms contracted) around the Fe and P atoms which leaves only the ammonium-1-hydroxypropylidene residues and the (P-)OH groups as ball and stick. Bridging phosphonate groups (P2 and P4) are shown with light grey faces, non-bridging phosphonates groups are drawn only with the outline of the tetrahedral skeleton.

$\Delta E_\mathrm{Q} = 2.27$ mm/s due to the second order Doppler effect. The observed large isomer shift $\delta^{\alpha-\mathrm{Fe}} > 1$ mm/s is indicative of Fe^{2+}, the large quadrupole splitting of the high spin state $(S = 2)$ [2, 12]. The iron atom is octahedrally coordinated by six oxygen atoms, four from two chelating bisphosphonate ligands and two from bridging phosphonate groups (Fig. 2).

Bond valence sum calculations for the iron atom of **1** based on the Fe–O distances give a value of 2.20, thereby supporting the +2 oxidation state [13, 14]. The hydrogen atoms of the hydrogenphosphonato groups and of the ammonium nitrogen atoms in **1** were found in the X-ray data Fourier maps and their atomic positions could be refined (although it was preferred to place the NH_3 protons in calculated positions). Furthermore, protonated O atoms are recognized by their longer P–O distance of 1.562 – 1.578 Å, versus 1.494 – 1.516 Å for unprotonated O atoms [11, 15]. Yet the occupation factors of the ten protic hydrogen atoms are closely related to the oxidation state of the iron atom. A full protic hydrogen occupation (1.0) of the two hydrogenphosphonato and ammonium groups translates into a single negative charge for each pamidronate ligand and, thus, an iron oxidation state of Fe(II). An Fe(III) compound would only require an average protic hydrogen occupation of 0.9. This small difference in hydrogen occupation will not be available from the structure refinement. Hence, the single-crystal X-ray structure refinement alone could not lead to an unambiguous formula assignment but needed the above Mößbauer evidence [2, 12]. Therefore, each zwitteri-

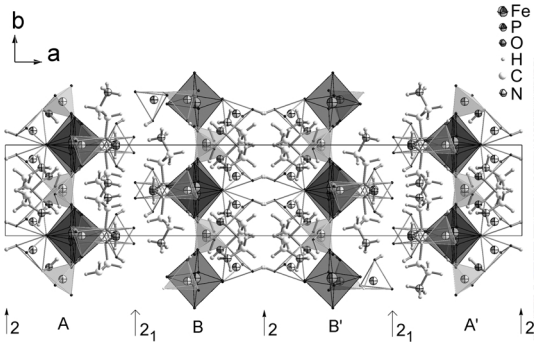

Fig. 4. Layer arrangement along *a*. The axes of rotation indicate the symmetry relationships between the layers. Hydrogen bonds between the layers are not shown for clarity. The building blocks A, B, B', and A' are emphasized.

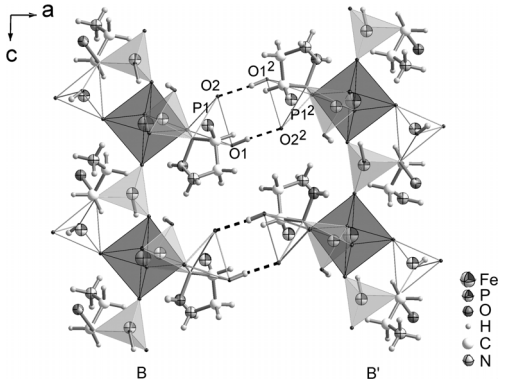

Fig. 5. Hydrogen bonding between B-B' or A-A' layers in the form of a complementary H-bond. Additional hydrogen bonds within the layers are not shown for clarity. O–H···O hydrogen bonding distances (Å) and angles (°): O1–H 0.83(8), H···O2^2 1.76(8), O1···O2^2 2.574(6), O1–H···O2^2 166(8); symmetry relation $2 = 1-x, y, 0.5-z$.

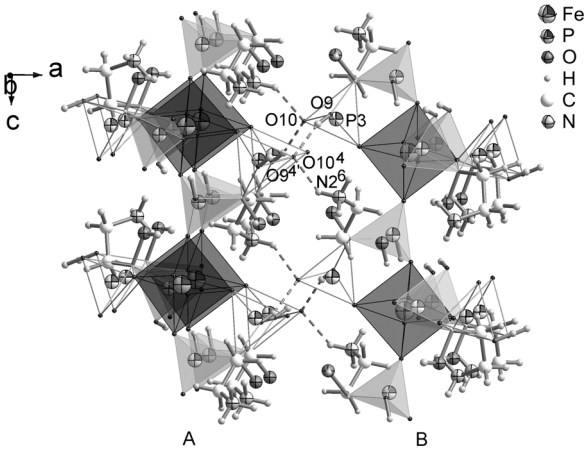

Fig. 6. Hydrogen bonding between A-B or A'-B' layers. Additional hydrogen bonds within the layers are not shown for clarity. O/N–H···O hydrogen bonding distances (Å) and angles (°): O9–H 0.70(8), H···O10^4 1.86(8), O9···O10^4 2.535(6), O9–H···O10^4 164(10), N2^6–H 0.90, H···O10^4 2.04, N2^6···O10^4 2.791(7), N2^6–H···O10^4 140.2; symmetry relations $4 = 0.5-x, 0.5+y, 0.5-z$, $6 = x, 1-y, 0.5+z$.

onic pamidronate anion was assigned as singly negative as depicted in Scheme 1 with each phosphonate group singly deprotonated to $-PO_2(OH)^-$ and the amino group protonated to an ammonium ion $-NH_3^+$.

The crystal structure of **1** is built from layers of alternating corner sharing $\{FeO_6\}$ octahedra and $\{PO_3C\}$ tetrahedra (Fig. 3 and 4). The layer can be described as a (4,4)- or 4^4-net, with iron being the node [16]. The layers lie parallel to the *bc*-plane and are stacked in an ABB'A' sequence along *a* due to the different hydrogen bonding interactions (see below). The non-bridging phosphonate groups are positioned above and below the plane which passes through the Fe atoms in Fig. 3.

Along *a* the layers are connected by hydrogen bonds between the non-Fe-bridging phosphonate groups to give a three-dimensional network. The hydrogen bonding interaction to each side of the layer is different. This creates a sequence of layers which can be described as ABB'A'. The relationship between B-B' or A-A' is by a two-fold rotation axis (2) parallel to *b* at (0 or 1/2, *y*, 1/4 or 3/4). Layers A-B or B'-A' are related by a two-fold screw axis (2_1) parallel to *b* at (1/4 or 3/4, *y*, 1/4 or 3/4). The hydrogen bonding between B and B' (or A and A') is depicted in Fig. 5. Between B and B' (or A and A') the non-bridging phosphonate groups of P1 are facing each other and give rise to a complementary H-bond between two symmetry related $-PO_2(OH)$-groups. This is different from the H-bonds between A and B (or B' and A') which is shown in Fig. 6. Between A and B (or B' and A') the non-bridging phosphonate groups of P3 are oriented towards each other. Here the hydrogen bonding between the $PO_2(OH)$-groups is not complementary but involves three phosphonate groups along *b*. In addition there is an N-H···O hydrogen bond. Additional O-H···O and N-H···O hydrogen bonds are formed within the layers (details are given in the deposited cif-file).

The structure of **1**, $^2_\infty[Fe(H_2PAM)_2]$, can be compared to those of the free zwitterionic acid, H_3PAM [17], the sodium monohydrate, $Na^+H_2PAM^-\cdot H_2O$ [11], the disodium pentahydrate, $2Na^+HPAM^{2-}\cdot 5\,H_2O$ [9], the calcium dihydrate,

$^1_\infty$[Ca(H_2PAM)$_2$]·2 H_2O [10] and the zinc aqua complex, [Zn(H_2PAM)$_2$(H_2O)$_2$] [18]. In all structures the pamidronate is present in its zwitterionic form. The calcium compound consists of one-dimensional metal-ligand columns which are extended to a three-dimensional hydrogen-bonded framework. Zinc pamidronate is built up from molecular complexes which are linked by H bonds. Noteworthy, in **1** the covalent metal-ligand dimensionality has been extended to a (4,4)-net, which we trace to the absence of additional water molecules of crystallization or aqua ligands. Crystals of calcium and zinc pamidronate were grown by solvent evaporation from water, while **1** was obtained by hydrothermal synthesis.

Experimental Section

General procedures

All work involving air- and/or moisture-sensitive compounds was carried out by using standard vacuum and Schlenk techniques. IR spectra (KBr pellet) were measured on a Bruker Optik IFS 25. NMR spectra were recorded with a Bruker Avance DPX200 spectrometer at 300 K (200 MHz for ^{1}H, 81 MHz for ^{31}P with ^{1}H broad band decoupling) with calibration against the solvent signal (D_2O 4.87 ppm) or an external standard of 85% H_3PO_4, respectively. Elemental analyses were obtained on a VarioEL from Elementaranalysensysteme GmbH. ^{57}Fe Mößbauer spectra were collected in constant acceleration mode with a ^{57}Co(Rh) source. The transmission of the γ-radiation was detected by a NaI(Tl) scintillation counter; velocity calibration was performed with an α-Fe foil at room temperature; spectra were fitted by Lorentzian lines.

The sodium salt of pamidronate, sodium (3-ammonium-1-hydroxypropylidene-1,1-bisphosphonate) monohydrate (=3-amino-1-hydroxypropylidene-1,1-bisphosphonic acid monosodium salt), Na[$H_3NCH_2CH_2C(OH)(PO_3H)(PO_3H)$]·$H_2O$, was prepared by the method of Kieczykowski and coworkers [19]. The product was collected by filtration, washed with cold water and 95% ethanol and dried at room temperature for one night (yield 9.0 g, 57%). IR (major peaks only): ν = 3300 (br, νOH), 1654 (νC–C), 1475 (νP=O), 1074 cm^{-1} (νP–O). – ^{1}H NMR (D_2O): δ = 3.43 (t, CH_2, J = 5.6 Hz), 2.38 (m, CH_2, J = 5.6 Hz). – ^{31}P NMR (D_2O): δ = 17.06. – $C_3H_{12}NO_8P_2Na$ (275.06): calcd. C 13.10, H 4.40, N 5.09; found C 12.45, H 4.54, N 4.62.

*Bis(3-ammonium-1-hydroxypropylidene-1,1-bisphosphonato)iron(II) (**1**)*

$FeCl_2 \cdot 4H_2O$ (0.30 g, 1.50 mmol) was dissolved in a Schlenk flask under a positive pressure of argon in 5 ml of degassed water to give a yellowish-green clear solution. To this solution sodium pamidronate monohydrate (0.83 g, 3.0 mmol) was added with continuous stirring. The pH value of the resulting solution was 3.1. The mixture was stirred at room temperature for 30 min. The solution was transferred to a Teflon-lined stainless steel autoclave and heated to 180 °C for 40 h followed by slow cooling at a rate of 10 °C/h. Brownish-red (violet) crystals were collected by filtration (yield 0.31 g, 39%). IR (major peaks only): ν = 3313 (br, νOH), 1650 (νC–C), 1482 (νP=O), 1104 cm^{-1} (νP–O). – $C_6H_{20}FeN_2O_{14}P_4$ (523.97): calcd. C 13.75, H 3.85, N 5.35; found C 14.19, H 4.54, N 4.30.

Crystal structure determination of **1**

Crystal data: Molecular formula $C_6H_{20}FeN_2O_{14}P_4$, formula weight 523.97 g mol^{-1}, a = 37.993(17), b = 6.680(3), c = 13.005(6) Å, β = 91.101(13)°, V = 3300(2) Å^3, Z = 8, D_{calc} = 2.109 g cm^{-3}, monoclinic, space group $C2/c$.

Data collection: Bruker Smart AXS CCD, Mo-K$_\alpha$ radiation (λ = 0.71073 Å), graphite monochromator, crystal size 0.20 × 0.11 × 0.03 mm^3, 233(2) K, ω-scan, 4.3° ≤ 2θ ≤ 50.7°, −45 ≤ h ≤ 45, −7 ≤ k ≤ 8, −15 ≤ l ≤ 15, 10297 reflections measured, 3005 independent (R_{int} = 0.0625), μ(Mo-K$_\alpha$) 1.383 mm^{-1}, F(000) 2144; data collection and cell refinement with SMART [20], data reduction with SAINT [20], experimental absorption correction with SADABS [21].

Structural Analysis and Refinement: The structure was solved by direct methods (SHELXS-97), refinement was done by full-matrix least squares on F^2 using the SHELXL-97 program suite [22]. All non-hydrogen positions were found and refined with anisotropic displacement parameters. The hydrogen atoms on the four crystallographically different hydrogenphosphonato groups were found from the difference Fourier map and their positions were refined isotropically with Ueq(H) = 1.5 Ueq(O). Hydrogen atoms on carbon, oxygen atoms of -COH and ammonium-nitrogen atoms were placed at calculated positions, using appropriate riding models (AFIX 23 for CH_2, AFIX 133 for NH_3 and AFIX 83 for -COH) and Ueq(H) = 1.2 Ueq(C) for CH_2 and Ueq(H) = 1.5 Ueq(N,O) for -COH and NH_3. 256 refined parameters, final $R1$ = 0.0542, $wR2$ = 0.1294 for 2099 reflections with $I > 2\sigma(I)$, final $R1$ = 0.0796, $wR2$ = 0.1374 for all data, goodness-of-fit 1.127, largest difference peak and hole 1.691/ − 0.749 e Å^{-3} in the vicinity (0.9/1.0 Å) of the P2/Fe atom. Graphics were obtained with DIAMOND (Version 3.0e) [23]. The structural data has been deposited with the Cambridge Crystallographic Data Center (No. CCDC-285961).

Acknowledgements

The research was supported by GABA Intl., Switzerland. We appreciate a fellowship to K.A-S. by the Graduate College "Unpaired electrons".

[1] G. Alberti, U. Constantino, M. Casciola, R. Vivani, Adv. Mater. **8**, 291 (1996); J. L. Snover, H. Byrd, E. P. Suponeva, E. Vicenzi, M. E. Thompson, Chem. Mater. **8**, 1490 (1996).

[2] K. Abu-Shandi, H. Winkler, B. Wu, C. Janiak, Cryst. Eng. Comm **5**, 180 (2003).

[3] R. Clarke, K. Latham, C. Rix, M. Hobday, J. White, CrystEngComm. **7**, 28 (2005); S. Midollini, A. Orlandini, A. Vacca, Inorg. Chem. Commun. **7**, 1113 (2004); B.-P. Yang, Z.-M. Sun, J.-G. Mao, Inorg. Chim. Acta **357**, 1583 (2004); M. Riou-Cavellec, M. Sanselme, G. Férey, J. Mater. Chem. **10**, 745 (2000).

[4] *Cobalt*: L.-M. Zheng, S. Gao, P. Yin, X.-Q. Xin, Inorg. Chem. **43**, 2151 (2004); P. Yin, S. Gao, L.-M. Zheng, X.-Q. Xin, Chem. Mater. **15**, 3233 (2003); P. Yin, S. Gao L.-M. Zheng, Z.-M. Wang, X.-Q. Xin, Chem. Commun. 1076 (2003).

[5] *Iron*: C. A. Merrill, A. K. Cheetham, Inorg. Chem. **44**, 5273 (2005); H.-H. Song, L.-M. Zheng, G.-S. Zhu, Z. Shi, S.-H. Feng, S. Gao, Z. Hu, X.-Q. Xin, J. Solid State Chem. **164**, 367 (2002); M. Riou-Cavellec, C. Serre, J. Robino, M. Noguès, J.-M. Grenèche, G. Férey, J. Solid State Chem. **147**, 122 (1999); L.-M. Zheng, H.-H. Song, C.-H. Lin, S.-L. Wang, Z. Hu, Z. Yu, X.-Q. Xin, Inorg. Chem. **38**, 4618 (1999); A. W. Herlinger, J. R. Ferraro, J. A. Garcia, R. Chiarizia, Polyhedron **17**, 1471 (1998).

[6] C. Janiak, Dalton Trans. 2781 (2003).

[7] W. R. Harris, C. E. Brook, C. D. Spilling, S. Elleppan, W. Peng, M. Xin, J. Van Wyk, J. Inorg. Biochem. **98**, 1824 (2004); E. Gumienna-Kontecka, J. Galezowska, M. Drag, R. Latajka, P. Kafarski, H. Kozlowski, Inorg. Chim. Acta **357**, 1632 (2004).

[8] Selected recent references: G. Duque, R. Segal, J. Bianco, J. Am. Geriatrics Soc. **53**, 1633 (2005); T. J. Cho, I. H. Choi, Y. C. Chung, J. Pediatric Orthopaedics **25**, 607 (2005); S. C. L. M. Cremers, S. E. Papapoulos, H. Gelderblom, J. Bone Mineral Res. **20**, 1543 (2005); A. N. Toukap, G. Depresseux, J. P. Devogelaer, LUPUS **14**, 517 (2005); J. M. Stephens, M. S. Aapro, M. F. Botteman, J. Clin. Oncol. **23**, 44S Part 1, Suppl. S (2005); J. Jung, G. Hwang, Y. Lee, J. Clin. Oncol. **23**, 99S Part 1 Suppl. S (2005).

[9] D. Vega, D. Fernández, J. A. Ellena, Acta Crystallogr. C **58**, m77 (2002).

[10] D. Fernández, D. Vega, A. Goeta, Acta Crystallogr. C **58**, m494 (2002).

[11] K. Stahl, S. P. Treppendahl, H. Preikschat, E. Fischer, Acta Crystallogr. E **61**, m132 (2005).

[12] K. Abu-Shandi, H. Winkler, M. Gerdan, F. Emmerling, B. Wu, C. Janiak, Dalton Trans. 2815 (2003).

[13] Bond valences (s) calculated from the bond lengths (R) according to $s = \exp(R_0 - R)/B$ and $R_0 = 1.734$ for Fe^{2+}–O, $B = 0.37$. Program VALENCE (Version 2.00, February 1993). I. D. Brown, J. Appl. Crystallogr. **29**, 479 (1996).

[14] I. D. Brown, R. D. Shannon, Acta Crystallogr. A **29**, 266 (1973); I. D. Brown, K. K. Wu, Acta Crystallogr. B **32**, 1957 (1976). I. D. Brown, D. Altermatt, Acta Crystallogr. B **41**, 244 (1985).

[15] E. Craven, K. Abu-Shandi, C. Janiak, Z. Anorg. Allg. Chem. **629**, 195 (2003).

[16] A. F. Wells, Structural Inorganic Chemistry, 5^{th} ed., Oxford Science Publications (1984).

[17] L. M. Shkol'nikova, S. S. Sotman, E. G. Afonin, Kristallografiya, **35**, 1442 (1990); L. M. Shkol'nikova, S. S. Sotman, E. G. Afonin, Sov. Phys. Crystallogr. **35**, 850 (1990).

[18] D. Fernández, G. Polla, D. Vega, J. A. Ellena, Acta Crystallogr. C **60**, m73 (2004).

[19] G. R. Kieczykowski, R. B. Jobson, D. G. Melillo, D. F. Reinhold, V. J. Grenda, I. Shinkai, J. Org. Chem. **60**, 8310 (1995).

[20] SMART, Data Collection Program for the CCD Area-Detector System; SAINT, Data Reduction and Frame Integration Program for the CCD Area-Detector System. Bruker Analytical X-ray Systems, Madison, Wisconsin, USA (1997).

[21] G. Sheldrick, Program SADABS: Area-detector absorption correction, University of Göttingen, Germany (1996).

[22] G. M. Sheldrick, SHELXS-97, SHELXL-97, Programs for Crystal Structure Analysis, University of Göttingen, Germany (1997).

[23] DIAMOND 3.0e for Windows. Crystal Impact Gbr, Bonn, Germany; http://www.crystalimpact.com/diamond.